Powder Technology 321 (2017) 55–65

Contents lists available at ScienceDirect

Powder Technology

journal homepage: www.elsevier.com/locate/powtec

Process analysis and global optimization for the microencapsulation of phytosterols by spray drying

Carla Agustina Di Battista [a,*], Diana Constenla [a], María Verónica Ramírez Rigo [a,b], Juliana Piña [a]

[a] Planta Piloto de Ingeniería Química, Departamento de Ingeniería Química, Universidad Nacional del Sur (UNS) – CONICET, Bahía Blanca, Argentina
[b] Departamento de Biología, Bioquímica y Farmacia, Universidad Nacional del Sur (UNS), Bahía Blanca, Argentina

ARTICLE INFO

Article history:
Received 7 March 2017
Received in revised form 19 July 2017
Accepted 6 August 2017
Available online 8 August 2017

Keywords:
Surface response methodology
Optimization
Spray drying
Phytosterols
Microencapsulation
Desirability

ABSTRACT

The response surface methodology (RSM) was used to optimize the microencapsulation of phytosterols by spray drying. The independent variables were drying air inlet temperature, atomization air flowrate, feed flowrate, phytosterols and total solids contents and the mass ratio between wall materials (Arabic gum and maltodextrin). The analyzed responses were process yield, mean volume particle size of product microparticles, phytosterols retention and encapsulation efficiency. Statistical analysis revealed that the selected independent variables, especially the atomization air flowrate and feed phytosterols content, significantly affect the studied responses. Taking into account the observed results and the analysis of variance, all the responses were successfully adjusted to second order models with interactions, showing good R^2 values and correlating the experimental data properly. The product microparticles were also obtained by using the predicted optimal operating and formulation variables to test the validity of the quadratic models. The experimental responses were found to be in agreement with the predicted values and were within the acceptable limits, indicating the suitability of the model for predicting key parameters related to process performance and product quality. The recommended optimal formulation and operating conditions for microencapsulation of phytosterols by spray drying are: drying air temperature of 160 °C, atomization air and feed flowrates of 498 L/h and 2.5 mL/min (equivalent to 42 mm of height of rotameter and 7% pump scale, respectively), phytosterols and total solids concentrations of 2 and 15 g/100 mL, respectively, and mass ratio between Arabic gum and maltodextrin of 2.06. The process yield, encapsulation efficiency and phytosterols retention obtained under the optimum conditions were 84, 72 and 76%, respectively. The product microparticles had a mean volume particle size of about 5 μm, well below the more restricted upper size limit of 25 μm required to guarantee the incorporation of PS into the intestine micellar phase.

1. Introduction

Phytosterols (PS) are vegetable sterols with a similar structure and functionality to cholesterol [1–3]. They are poorly absorbed into the blood stream [4,5], but are widely recognized as lowering absorption of cholesterol and their serum levels [6]. It has been found that PS do not need to be dissolved to exert their hypocholesterolemic effect, it is sufficient if they are dispersed [7]. Indeed, the PS must be administered finely divided in order to facilitate their exposure to the bile salts (particle size about 25 μm) [7], and to reduce the sandy mouth feel (particle size about 50 μm) [8].

Taking into account their hypocholesterolemic effects, the use of phytosterols in food has been explored for the prevention and treatment of cardiovascular diseases, among other affections. In this context, one of the most attractive challenges is their incorporation in aqueous-based formulations (like beverages, soups and others). Definitely, the hydrophobic and water insoluble nature of PS make them poor candidates for stable dispersions and hinder their applicability on these type of intermediate or final products [9].

Microencapsulation is a common technique used to provide a physical barrier (composed by wall materials) between the active ingredient (called core) and the other components of the product [10]. Among other methods, spray drying has been successfully applied for encapsulation of food ingredients because it allows to produce particles of high quality and stability by means of a relatively flexible, simple, low-cost and continuous process [11,12]. This technique consists in the atomization of a solution or liquid suspension into tiny drops, followed by drying in a stream of hot air to produce solid microparticles [13].

In spray drying, both formulation and process parameters become important to achieve the desired characteristics in the powdered product. Firstly, the liquid feed preparation plays an essential role in the content of the encapsulated ingredient in the final powder [14]. Specifically, the most significant parameters are the core content and total solids concentration (including the wall materials and their composition) [14–16]. Other factors to be considered in the

* Corresponding author.
E-mail address: adibattista@plapiqui.edu.ar (C.A. Di Battista).

http://dx.doi.org/10.1016/j.powtec.2017.08.008
0032-5910/

microencapsulation by spray drying are the feed interfacial properties, which can be addressed by using surfactants [17–19].

Secondly, the operating conditions depend on the characteristics of the feed suspension and on the desired product properties [20]. In this context, optimal drying conditions (as feed and atomization air flowrate, inlet temperature of drying air, among others) must be considered in order to minimize the non-encapsulated core material in the product [14,16,21].

Regarding the microencapsulation of phytosterols by spray drying, Di Battista et al. [19] studied the effect of the use of Arabic gum (AG) and maltodextrin (MD) as wall materials, and the influence of the addition of surfactants on feed properties, particle size of product microparticles and process performance (process yield, microencapsulation efficiency and phytosterols retention).

In this context, the aim of this work is to study the influence of formulation and operating variables on the product microparticles size and process performance. Particularly, and by means of a Box-Behnken experimental design, the effect of several factors (drying air inlet temperature, X_1; atomization air flowrate, X_2; feed flowrate, X_3; phytosterols content, X_4; total solids content, X_5; and mass ratio between the wall materials AG/MD, X_6) on different key product and process parameters (process yield, Y_1; mean particle size of product microparticles, Y_2; phytosterols retention, Y_3 and encapsulation efficiency, Y_4) was analyzed. By using response surface methodology (RSM), a statistical model was fitted for each response as a function of the independent factors. Finally, the models were combined in order to find an optimum set of conditions that improves the product and process responses simultaneously. In order to evaluate the final product, the stability of the powder obtained under optimal conditions was tested in 2 aqueous systems (water at room temperature and an instant fruit drink powder).

2. Materials and methods

2.1. Materials

Phytosterols powder and Arabic gum were supplied by Grupo Saporiti (Buenos Aires, Argentina). The PS powder consisted in a mixture of β-sitosterol (35–55% w/w), campesterol (18–27% w/w), stigmasterol (21–35% w/w) and about of 0–7% w/w of other vegetable sterols. Maltodextrin Globe® 019150 (DE 15) was supplied by Todo Droga (Córdoba, Argentina). The phytosterols, Arabic gum and maltodextrin were food grade. The pro-analysis grade surfactant, sodium dodecyl sulfate (SDS) (HLB 40, molecular weight 289) was supplied by Cicarelli® Reagents S.A. (Santa Fe, Argentina). A commercial orange flavored fruit juice powder (Clight, Mondelēz International) was used for the physical stability study.

2.2. Methods

2.2.1. Preparation of the liquid feed and the product microparticles

The liquid feed to be spray dried was prepared following the procedure described by Di Battista et al. [19]. Briefly, Arabic gum and maltodextrin were dispersed at different mass ratios (as detailed in Table 1) and dissolved in 100 mL of hot distilled water (50 °C) under magnetic stirring for about 30 min. Then, 2 g of SDS were added to form the wall solutions. Finally, PS were dispersed at different concentrations (Table 1) under continuous agitation for 1 h, reaching the total solids contents (based on the sum of AG, MD, SDS and PS masses) reported in Table 1. The recently formed suspensions were homogenized using a Pro II Homogenizer at room temperature, over 9 min at 25000–35000 rpm, and sonicated for 60 s to remove the foam and aggregates.

The product microparticles were obtained by spray drying the suspensions, using a co-current Mini Spray Dryer Büchi B-290 (Büchi Labortechnik AG, Flawil, Switzerland), provided with a two-fluid nozzle with a cap orifice diameter of 0.5 mm. During atomization, the suspensions were kept agitated at 800 rpm and ambient temperature.

Table 1
Factors and responses for the Box-Behnken experimental design.

Independent factors	Levels			Units
	Low (−)	Medium (0)	High (+)	
X_1: Drying air inlet temperature (T_{in})	110	135	160	°C
X_2: Atomization air flowrate (Q_{atom})	30	45	60	mm
X_3: Feed flowrate (Q_{feed})	5	10	15	%
X_4: PS content ($Cont_{PS}$)	2	5	8	g/100 mL
X_5: Total solids content ($Cont_{TS}$)	15	25	35	g/100 mL
X_6: Mass ratio AG to MD (AG/MD)	1/19	9.5263	19/1	–

Responses	Units	Optimum
Y_1: Process yield (PY)	%	Maximum
Y_2: Mean particle size of product ($D\,[4,3]_{Part}$)	μm	Minimum
Y_3: Phytosterols retention (PR)	%	Maximum
Y_4: Encapsulation efficiency (EE)	%	Maximum

Table 1 shows the process and formulation conditions, which were defined following the design of experiments detailed below and using a drying air flowrate about 38 m^3/h.

2.2.2. Design of experiments for response surface methodology

Response surface methodology (RSM) was employed in order to investigate the effect of different operating and formulation variables (including atomization air and feed flowrates, inlet temperature, PS and total solids concentration, and mass ratio between the wall materials) on the main responses of the phytosterols microencapsulation. The 6 factors were evaluated at 3 levels in a Box-Behnken design of experiments. Table 1 shows the independent factors (coded as X) and their proposed levels for analysis, together with the evaluated responses (coded as Y) and the objective of optimization for each one. As a result of the design, fifty four randomized experimental settings were generated, including 48 design points and 6 repetitions at the central point. The coded experimental settings are presented in Table 2.

2.2.3. Statistical analysis and modeling

The design of experiments was statistically analyzed using a significance level at 5% ($\alpha = 0.05$) to establish the main factors affecting the responses. After that, a quadratic polynomial regression model was assumed for predicting each Y variable as follows:

$$Y\prime_m = a_{0,m} + \sum_{i=1}^{i=k} a_{i,m}X_i + \sum_{\substack{i=1\\ j=1}}^{\substack{i=k\\ j=k}} a_{ij,m}X_iX_j \quad (1)$$

where Y'_m is the adjusted response (m), $a_{0,m}$ the constant, $a_{i,m}$ the linear coefficient and $a_{ij,m}$ the quadratic or interaction term, respectively for the response m; while X_i and X_j are the independent variables (inlet temperature, feed and atomization air flowrates, PS and total solids contents and AG/MG mass ratio) (Table 1).

The adjusted model for each response was judged in terms of the determination coefficient (R^2), the p-value of the model (p_{MOD}) and the p-value of the lack of fit test (p_{LOF}). Moreover, graphical tools were used in order to determine the model goodness. Namely, the normal distribution of residues (differences between the adjusted and experimental value, $Y_{l,m}$ - $Y'_{l,m} = r_{l,m}$ for each run l and response m), the adjusted versus experimental values ($Y'_{l,m}$ versus $Y_{l,m}$ for each run l and response m), the residues versus adjusted value ($r_{l,m}$ versus $Y'_{l,m}$ for each run l and response m), versus each factor value ($r_{l,m}$ versus X_i) and versus run number ($r_{l,m}$ versus n_l). All models were adjusted guaranteeing the normal distribution of residues, the absence of patterns in the last three graphs and a good distribution in the adjusted versus experimental data graph.

Table 2
Experimental settings given by the Box-Behnken design, and results obtained for each run and response. Minimum and maximum values for each response are highlighted in bold.

No	X_1	X_2	X_3	X_4	X_5	X_6	Y_1	Y_2	Y_3	Y_4
1	−	0	+	0	0	+	51.31	8.326	39.57	23.37
2	0	0	+	−	0	+	61.59	9.382	32.91	39.69
3	0	+	+	0	+	0	47.94	7.14	37.16	39.84
4	+	−	0	+	0	0	43.28	15.479	32.04	**9.88**
5	0	0	0	0	0	0	60.24	8.858	50.16	24.59
6	0	0	+	+	0	+	54.27	9.42	42.78	15.71
7	0	+	0	0	+	−	61.22	9.27	46.82	27.6
8	0	+	−	0	−	0	70.27	8.058	50	32.24
9	−	−	0	−	0	0	37.56	10.418	33.52	57.42
10	−	0	0	+	−	0	59.58	10.945	43.42	56.7
11	−	0	−	0	0	+	55.5	7.693	48.58	34.18
12	−	0	0	−	+	0	49.66	9.456	48.02	63.62
13	0	−	+	0	−	0	39.67	10.328	34.75	29.93
14	0	0	0	0	0	0	55.14	8.697	49.26	26.38
15	0	−	+	0	+	0	26.53	12.345	**20.5**	22.59
16	0	+	+	0	−	0	58.1	7.98	46.15	38.19
17	0	+	0	0	−	+	71.51	7.444	61.24	36.13
18	−	0	+	0	0	−	63.73	9.892	48.85	23.95
19	0	−	0	0	+	−	44.94	8.301	32.62	23.41
20	+	−	0	−	0	0	48.61	8.546	48.45	65.92
21	+	0	+	0	0	−	66.26	9.188	47.67	38.05
22	0	0	0	0	0	0	62.37	8.142	51.94	21.06
23	0	−	−	0	+	0	39.91	10.292	35.51	30.99
24	0	0	+	+	0	−	61.99	12.187	44.2	30.32
25	−	+	0	−	0	0	59. 70	6.874	45.8	42.2
26	+	0	0	−	+	0	58.14	6.252	53.41	55.55
27	0	+	0	0	−	−	74.98	11.61	62.73	50.34
28	+	0	+	0	0	+	68.82	7.846	68.69	38.78
29	0	−	0	0	+	+	34.87	10.986	30.39	37.77
30	0	0	+	−	0	−	79.17	6.397	71.98	**78.06**
31	0	0	−	+	0	+	62.06	8.998	50.33	45.14
32	0	0	0	0	0	0	63.73	8.312	61.13	44.14
33	+	0	0	+	+	0	58.09	9.518	48.49	27.39
34	0	−	0	0	−	+	51.86	10.032	47.55	30.9
35	0	0	−	−	0	+	71.33	6.277	67.43	54.67
36	0	−	0	0	−	−	41.45	10.65	34.24	36.03
37	−	0	0	−	−	0	80.04	6.186	74.94	55.66
38	+	0	0	+	−	0	71.64	12.31	62.32	62.74
39	0	+	−	0	+	0	59.47	7.023	51.14	37.92
40	0	−	−	0	−	0	60.82	11.486	51.04	43.92
41	0	0	0	0	0	0	65.18	8.756	59.79	41.73
42	−	0	−	0	0	−	73.22	10.335	50.6	21.62
43	+	0	0	−	−	0	81.7	**6.083**	76.1	50.83
44	+	0	−	0	0	+	66.24	11.708	**85.56**	51.16
45	−	0	0	+	+	0	53.32	9.041	42.5	38.95
46	0	0	−	+	0	−	68.61	8.696	49.47	55.81
47	−	+	0	+	0	0	55.53	8.354	44.86	50.27
48	+	+	0	−	0	0	61.8	6.362	57.08	55.59
49	−	−	0	+	0	0	**25.2**	**16.717**	29.66	49.91
50	+	0	−	0	0	−	71.75	9.318	57.91	44.13
51	0	0	0	0	0	0	65.12	8.401	63.04	32.36
52	+	+	0	+	0	0	59.44	7.221	46.76	32.72
53	0	+	0	0	+	+	56.53	6.549	48.19	43.15
54	0	0	−	−	0	−	**86.72**	6.381	66.21	70.33

2.2.4. Particle size distribution and mean size of product microparticles

The product particle size distribution (PSD) was measured by laser light diffraction using a Horiba LA-950 V2 device (Irvine, United States). The refractive index used for statistical calculation of the particle size was 1.358 and three repetitions were realized for each sample. By averaging three repetitions, mean particle size was expressed as D [4,3], i.e. mean volume particle size.

2.2.5. Process yield

The process yield (PY) was gravimetrically determined as the ratio of the amount of powder collected after every spray-drying experiment, to the initial amount of solids contained in the feed suspensions:

$$PY\ [\%] = \frac{\text{Mass of powder collected } [g]}{\text{Mass of solids fed } [g]} \cdot 100\% \quad (2)$$

2.2.6. Encapsulation efficiency

The encapsulation efficiency (EE) is defined as the ratio between the encapsulated and total phytosterols in the spray-dried product:

$$EE\ [\%] = \frac{TP - FP}{TP} \cdot 100\% = \frac{\text{Mass of encapsulated phytosterols } [g]}{\text{Mass of total phytosterols collected } [g]} \cdot 100\% \quad (3)$$

where TP and FP are the amount of total and free (non-encapsulated) phytosterols in the microparticles, respectively. Both TP and FP were determined by solvent extraction, following the methodology described below [22].

2.2.6.1. Total content of phytosterols. For quantification of total amount of phytosterols presents in product, 4 g of microparticles was dispersed in 40 mL of distilled hot water (65 °C). After stirring gently, 8 mL of 25% NH_4OH were added and the suspension was kept at 65 °C for 20 min in a shaking water bath. Then, the suspension was cooled at room temperature and the lipids were extracted in a separator funnel applying three liquid–liquid extractions: first, 20 mL of ethanol, 50 mL of ethyl ether and 50 mL of n-hexane; second, 10 mL of ethanol, 50 mL of ethyl ether and 50 mL of n-hexane; and, third, 50 mL of ethyl ether and 50 mL of n-hexane. In each extraction step, the solvents were added successively with shaking between additions. The upper phase was collected and filtered through a Whatman 42 filter paper containing anhydrous Na_2SO_4, and then evaporated and dried to constant weight under nitrogen stream. The total content of phytosterols (TP) was expressed as:

$$TP\ [\%] = \frac{\text{Mass of total phytosterols collected } [g]}{\text{Mass of total solids collected } [g]} \cdot 100\% \quad (4)$$

2.2.6.2. Free content of phytosterols. The free phytosterols fraction was extracted by stirring 5 g of microparticles in a volume of 200 mL of n-hexane, during 15 min at room temperature and filtrated through a Whatman 42 filter paper. The solvent of filtrate was evaporated in a rotary evaporator (at 60 °C and 0.200 kg/cm^2 approximately) and the extract (free phytosterols) was dried to constant weight under nitrogen stream. The free content of phytosterols (FP) was expressed as:

$$FP\ [\%] = \frac{\text{Mass of free phytosterols collected } [g]}{\text{Mass of total solids collected } [g]} \cdot 100\% \quad (5)$$

2.2.7. Phytosterols retention

The phytosterols retention (PR) is the ratio between the amount of total phytosterols in the spray-dried product (encapsulated and free) and the amount of phytosterols fed in the aqueous suspension.

$$PR\ [\%] = \frac{\text{Mass of total phytosterols collected } [g]}{\text{Mass of phytosterols fed } [g]} \cdot 100\% \quad (6)$$

2.2.8. Optimization

Once the experimental data and fitting coefficients for each response were obtained, all the models were combined in a unique function (called "desirability") in order to find the better set of conditions that simultaneously improves all the response within the explored domain (i.e. the set of conditions that maximize the process yield, phytosterols retention and encapsulation efficiency, and minimize the mean volume particle size). All the independent variables were kept within the established ranges, while the responses were maximized or minimized according to the process/product requirements (Table 1).

The general approach for the desirability function is to transform the response (Y_i) into a dimensionless individual desirability function (d_i),

defined between 0 (completely undesirable response) and 1 (fully desirable response). Therefore, the overall desirability function (D) is defined as:

$$D = (d_i)^{1/m} \quad (7)$$

where m is the total number of responses taken into consideration.

2.2.9. Particle morphology and physicochemical characterization of optimum powder of microparticles

Particle morphology was assessed using an EVO 40-XVP, LEO Scanning Electron Microscope (SEM) (Oberkochen, Germany). Previously, the obtained powder was dried under air flow on a porthole and metalized with gold in a PELCO 91000 sputter coater (Tedpella, United States).

Moreover, in order to ensure the physicochemical stability of the phytosterols in the microparticle, differential scanning calorimetry (DSC), X-ray diffraction (XRD), Fourier transformed infrared spectroscopy (FTIR) and gas chromatography (GC) of the powder obtained under optimal conditions were performed. Details of these techniques and results are presented in the Supplementary material section.

2.2.10. Stability

The stability of the redispersed optimal microparticles was analyzed by means of turbidimetry using a Turbiscan MA 2000 (Formulaction SA, L'Union, France). The obtained longitudinal profiles of backscattered and transmitted light were referred to the initial state (scan taken at time 0) and are presented in the Supplementary material section.

The sample was prepared by dispersing 0.2 g of microparticles in 60 mL of an aqueous system (water at room temperature and a fruit drink beverage prepared by dissolution of instant powder). An aliquot of 8 mL of the dispersed sample was placed into the tube. The scanning period was 120 days for the water system and 2 days for the instant beverage. The instant beverage without the phytosterols microparticles and a suspension of raw phytosterols were also analyzed. Destabilization phenomena and phases' thickness were identified by analyzing the temporal evolution of the longitudinal profiles of transmitted and backscattered percentages.

3. Results and discussions

Once the 54 experiments were carried out (see results in Table 2), the effect of each independent variable and interactions between them were analyzed. Table 3 shows the p-value of all the source of variations for the studied responses. The individual analysis is presented below.

3.1. Process yield (Y_1)

The process yield was between 25.20% (run 49) and 86.72% (run 54). For this response all the independent factors had significant linear effects. Moreover, the quadratic effects (except for the feed flowrate) were significant (Table 3). The interactions between the inlet temperature, phytosterols content and total solids contents with AG/MD mass ratio were also significant on the process yield. Another significant interaction affecting this response was that between the total solids and phytosterols contents.

Table 4 shows the regression coefficients for the fitted model, which represents the experimental process yields as a function of the independent factors and their interactions. The obtained R^2 was 96.14% and the model did not show lack of fit ($p_{LOF} > 0.05$), ensuring that the fitted model was appropriate for adjusting the experimental data.

Process yield was improved at high atomization air flowrates and high inlet temperatures (Fig. 1a). Firstly, it is known that high atomization energy (here translated as flowrate) leads to lower mean droplet/particle sizes, increasing the total specific surface area [10,15] and, thus, the heat and mass transfer. Zhang & Youan [23] found similar results in the nanoencapsulation of oily compounds. The authors showed that a lower droplet drying time (which is linearly related to the droplet size) leads to a more efficient process in terms of yield. Moreover, when

Table 3
p-Values for the selected responses. Significant p-values (<0.05) are highlighted in bold.

Source	Y_1	Y_2	Y_3	Y_4
	p-Value	p-Value	p-Value	p-Value
X_1	**0.0000**	**0.0030**	**0.0276**	0.4851
X_2	**0.0000**	**0.0000**	**0.0036**	0.2641
X_3	**0.0000**	0.9518	0.0864	**0.0041**
X_4	**0.0094**	**0.0000**	**0.0048**	**0.0001**
X_5	**0.0000**	**0.0009**	**0.0039**	0.1082
X_6	**0.0008**	**0.0055**	0.7009	0.4096
X_1X_1	**0.0013**	**0.0129**	0.6224	0.4955
X_1X_2	0.0511	**0.0001**	0.8812	0.2655
X_1X_3	0.1701	0.3875	0.6776	0.4028
X_1X_4	0.1191	0.0565	0.9372	0.0618
X_1X_5	0.1818	0.8317	0.7612	0.5076
X_1X_6	**0.0224**	**0.0003**	0.1524	0.5143
X_2X_2	**0.0000**	**0.0000**	**0.0009**	0.4973
X_2X_3	0.3334	**0.0302**	0.9673	0.2207
X_2X_4	0.5355	**0.0006**	0.7456	0.0587
X_2X_5	0.0947	**0.0056**	0.3804	0.6050
X_2X_6	0.3185	**0.0000**	0.8775	0.7428
X_3X_3	0.6459	0.0639	0.3964	0.6628
X_3X_4	0.9078	**0.0304**	0.6021	0.1829
X_3X_5	0.2240	**0.0105**	0.3851	0.9477
X_3X_6	0.9359	0.0823	**0.0374**	0.2508
X_4X_4	**0.0000**	0.4222	0.9746	**0.0001**
X_4X_5	**0.0000**	**0.0180**	0.2104	**0.0075**
X_4X_6	**0.0000**	**0.0001**	0.0608	0.1605
X_5X_5	0.1335	**0.0000**	0.6114	0.1866
X_5X_6	**0.0124**	**0.0066**	0.8344	0.0565
X_6X_6	**0.0000**	0.7381	0.6741	0.3706

Table 4
Regression coefficients of the models for the selected responses.

Regression coefficients	Y_1	Y_2	Y_3	Y_4
a_0	−134.5100	45.6856	−102.8590	159.0940
a_1	1.4282	−0.4152	0.8908	−0.5117
a_2	7.6110	−0.9181	5.1242	−1.6936
a_3	−0.4059	0.0166	5.8425	−0.2089
a_4	−16.8733	2.1208	−7.5705	−8.5319
a_5	−1.9995	0.5519	−1.5524	−0.5022
a_6	−3.3262	−0.2358	−2.7425	−3.2035
a_{11}	−0.0054	0.0009	−0.0023	0.0027
$a_{12} = a_{21}$	−0.0057	0.0036	−0.0014	0.0091
$a_{13} = a_{31}$	0.0113	−0.0015	−0.0105	−0.0185
$a_{14} = a_{41}$	0.0159	0.0045	−0.0025	−0.0555
$a_{15} = a_{51}$	0.0058	−0.0002	−0.0040	−0.0077
$a_{16} = a_{61}$	0.0104	0.0040	0.0200	0.0077
a_{22}	−0.0639	0.0077	−0.0546	−0.0078
$a_{23} = a_{32}$	−0.0152	−0.0074	−0.0018	0.0504
$a_{24} = a_{42}$	0.0146	−0.0229	0.0250	0.1354
$a_{25} = a_{52}$	−0.0084	−0.0031	0.0139	0.0073
$a_{26} = a_{62}$	−0.0066	−0.0075	−0.0036	−0.0069
a_{33}	−0.0177	0.0151	−0.1009	0.0450
$a_{34} = a_{43}$	−0.0081	−0.0353	−0.1054	−0.2404
$a_{35} = a_{53}$	−0.0288	0.0137	−0.0585	0.0039
$a_{36} = a_{63}$	0.0012	0.0061	−0.1045	−0.0472
a_{44}	0.6463	0.0179	0.0101	1.5519
$a_{45} = a_{54}$	0.1780	−0.0196	0.1428	−0.2970
$a_{46} = a_{64}$	0.2708	−0.0399	0.2178	0.1374
a_{55}	0.0141	−0.0106	0.0152	0.0349
$a_{56} = a_{65}$	−0.0265	0.0060	−0.0073	0.0650
a_{66}	0.0660	−0.0007	0.0138	0.0261
R^2	96.14	93.83	77.87	72.65
p_{MOD} *	0.0000	0.0000	0.0000	0.0005
p_{LOF} **	0.0647	0.1054	0.7556	0.0909

* p_{MOD}: p-value of the model.
** p_{LOF}: p-value of the lack of fit test.

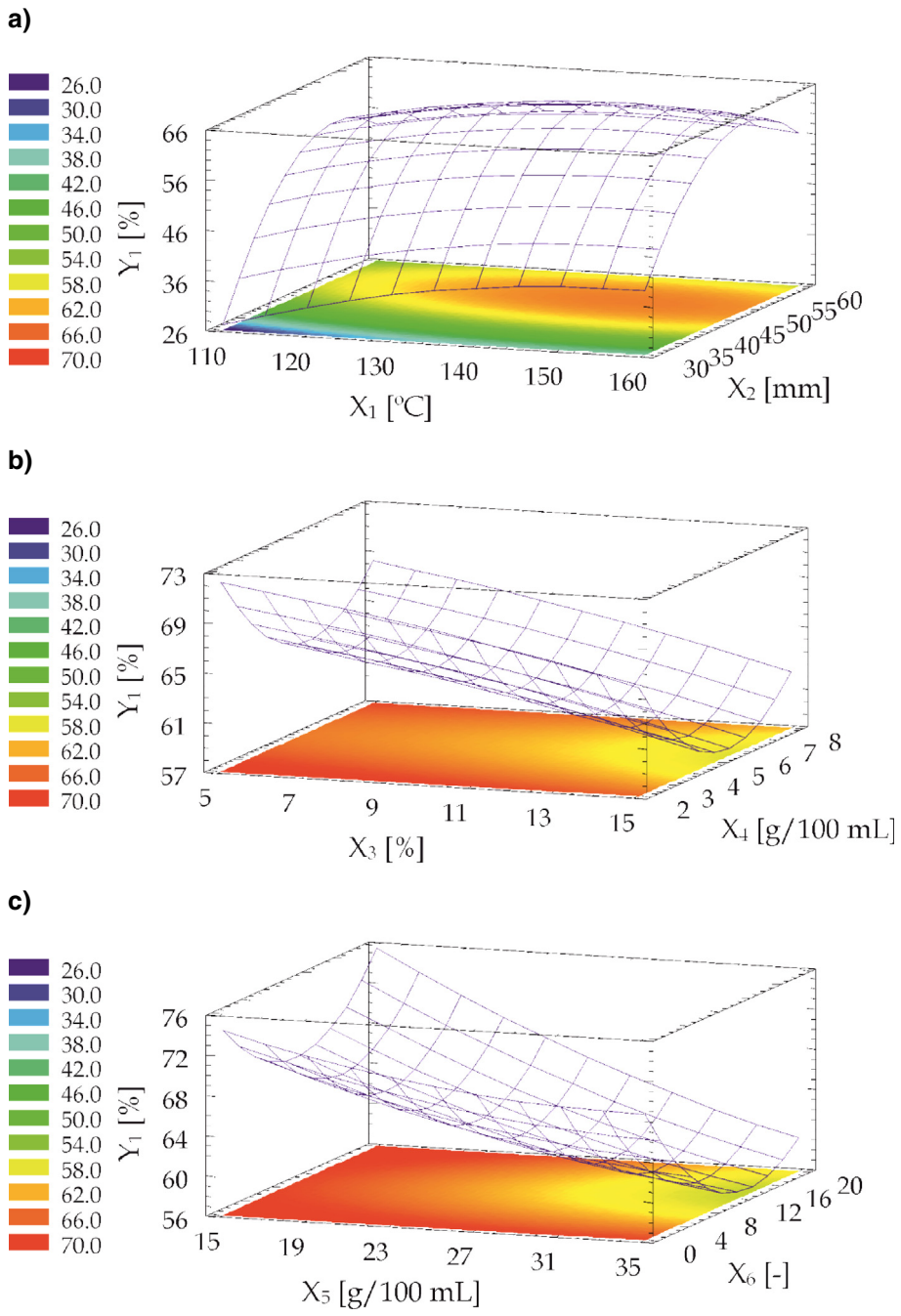

Fig. 1. Response surface plots showing the variation of the process yield against: a) inlet temperature (X_1) and air atomization flowrate (X_2); b) feed flowrate (X_3) and phytosterols content (X_4); c) total solids content (X_5) and AG to MD mass ratio (X_6).

lower droplet sizes are generated, the atomization cone is narrower, reducing their probability of reaching the drying chamber walls and, thus diminishing losses by sticking [24].

However, the quadratic effect showed that at very high atomization air flowrates, the process yields were slightly reduced; probably as a consequence of an excessive diminution in the droplet sizes, which leads to increase in the drag of particles by the exhaust air.

Secondly, it is well known that the inlet temperature also affects droplets drying. Effectively, water evaporation is improved at high drying temperatures due to better heat and mass transfer, and then, the process yield is enhanced. Several authors reported equivalent results for the spray drying of different materials [25–28].

Fig. 1b shows the effects of the feed flowrate (X_3) and phytosterols content (X_4) on the process yield. As it can be seen in Table 3, the linear term of X_3 was significant on this response. Certainly, an increase in the feed flowrate leads to an unsuccessful drying of the droplets/particles due to the reduction in both the mass ratio between the air and feed flowrates [23] and the contact time between the droplets/particles and drying air [29]. Therefore, the higher process yields for lower X_3 values are explained by a higher capacity of water evaporation and, thus, a lower probability of droplets/particles sticking on the chamber walls. Kaur et al. [30] and Roccia et al. [27] observed similar results in the spray drying of solid dispersions and sunflower oil encapsulation, respectively.

As reported in Table 3, the linear term of the total solids content (X_5) is one of the most significant factors affecting the process yield. This response diminishes by increasing X_5 (see Fig. 1c) as a consequence of an increment in the suspension viscosity, which promotes sticking on the

chamber walls [10,19,31]. This effect was also observed by Tonon et al. [28] during the spray drying of açai, and by Tontul & Topuz [32] in the production of linseed oil powders.

The quadratic term of phytosterols content (X_4) and AG to MD mass ratio (X_6) also showed a significant impact on the process yield. The process yield was enhanced at low values of both factors. The effect of low phytosterols content can also be explained by the decrease in the suspension viscosity, which increases the process yield. On the other hand, this response could be improved by the higher surface tensions provided by lower AG proportions [33].

3.2. Mean volume size of product microparticles (Y_2)

The mean volume size of the product microparticles was between 6.083 μm (assay 43) and 16.717 μm (assay 49), corresponding to formulations with low and high phytosterols contents, respectively (Table 2).

With the exception of the feed flowrate (X_3), all the main effects and their interactions with the atomization air flowrate (X_1X_2, X_2X_4, X_2X_5 and X_2X_6) and with the AG to MD ratio (X_1X_6, X_4X_6, X_5X_6 and X_2X_6) were significant on this response (Table 3). Moreover, Table 3 shows that the mean volume particle size was affected also by the interactions between total solids contents and feed flowrate (X_3X_5), and between contents of total solid and phytosterols (X_4X_5). Furthermore, the inlet temperature, atomization air flowrate and total solids contents had significant quadratic effects.

Table 4 also shows the regression coefficients for the model of the mean volume particle size. The data variability was explained by the model at 93.83% (R^2); whereas the p-value was lower than 0.05. Furthermore, the obtained model did not show lack of fit ($p_{LOF} > 0.05$).

Fig. 2 shows the adjusted response surfaces for the mean volume particle size as a function of the independent factors. In accordance with [10], the mean particle size is directly related with the physicochemical changes that the particles undergo during drying. At low

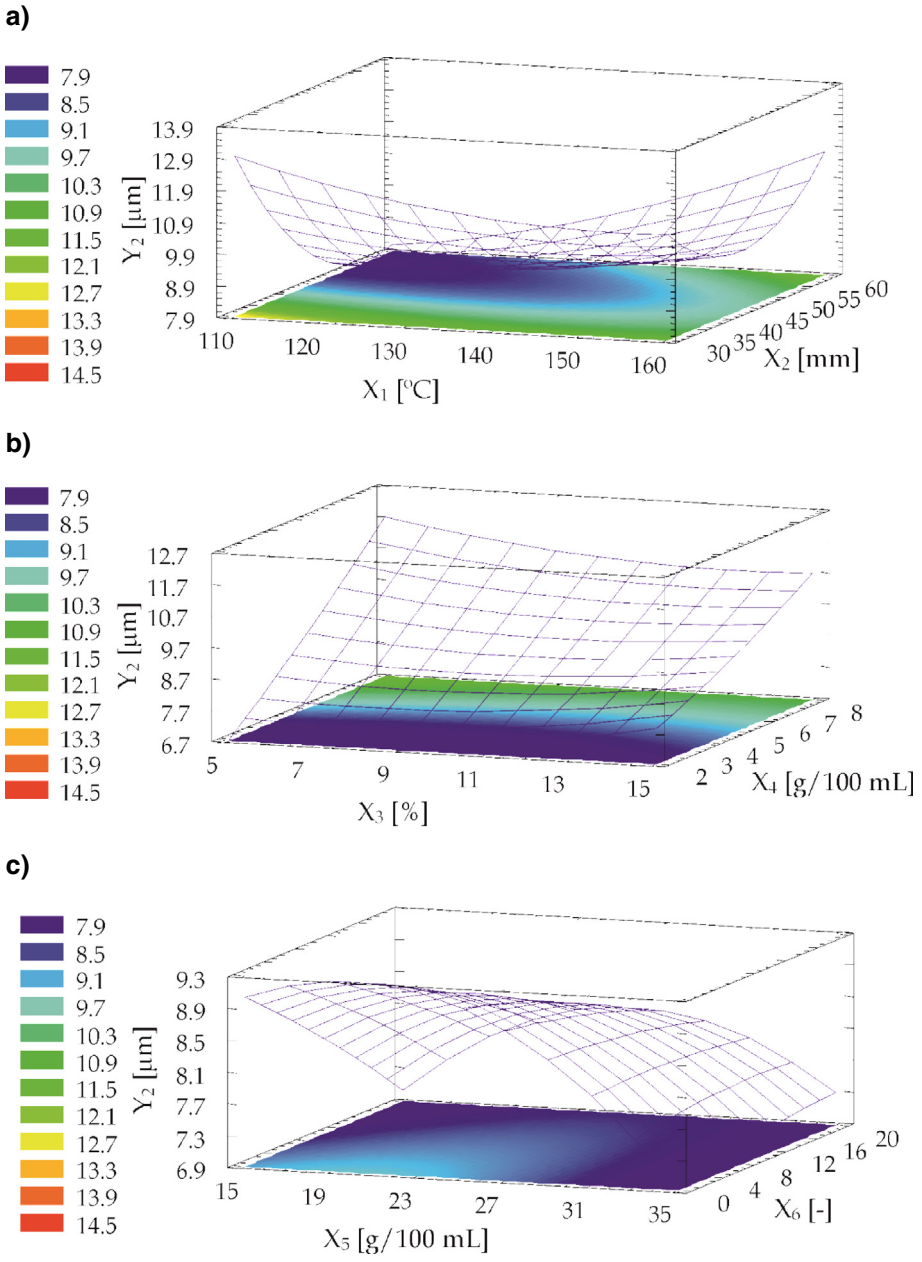

Fig. 2. Response surface plots showing the variation of the mean volume size for the product microparticles against: a) inlet temperature (X_1) and air atomization flowrate (X_2); b) feed flowrate (X_3) and phytosterols content (X_4); c) total solids content (X_5) and AG to MD mass ratio (X_6).

temperatures, a slight increase in this factor decreased the mean product particle size (Fig. 2a). This effect can be attributed to a diminution in the feed surface tension and viscosity, which allow the atomization in tiny droplets and, then, the production of smaller microparticles. Gallo et al. [34] and Mishra et al. [35] found similar effects in the spray drying of *Rhamnus purshiana* and *Emblica officinalis*, respectively.

Nevertheless, at high temperatures, the effect was opposite, i.e. the mean volume particle size increased as a consequence of the inflation phenomenon promoted by high temperatures. Moreover, under these conditions drying could take place suddenly, avoiding the typical particle shrinkage [36,37].

One of the most significant factors on the mean volume size of the product microparticles was the atomization air flowrate (at linear and quadratic terms) (Fig. 2a). As above mentioned, lower mean droplet sizes can be achieved by increasing the atomization air flowrate, favoring the formation of more fine particulate product [15,24,34]. Nevertheless, an increase in the mean particle size at high atomization air flowrates was observed. This can be explained by the fact that the finest particles tend to be dragged by the exhaust air downstream to the cyclone, decreasing the process yield.

As expected, the main factor affecting the mean particle size was the phytosterols content in the feed suspension. Indeed, an increase in the PS concentration led to an increase in the mean size of product

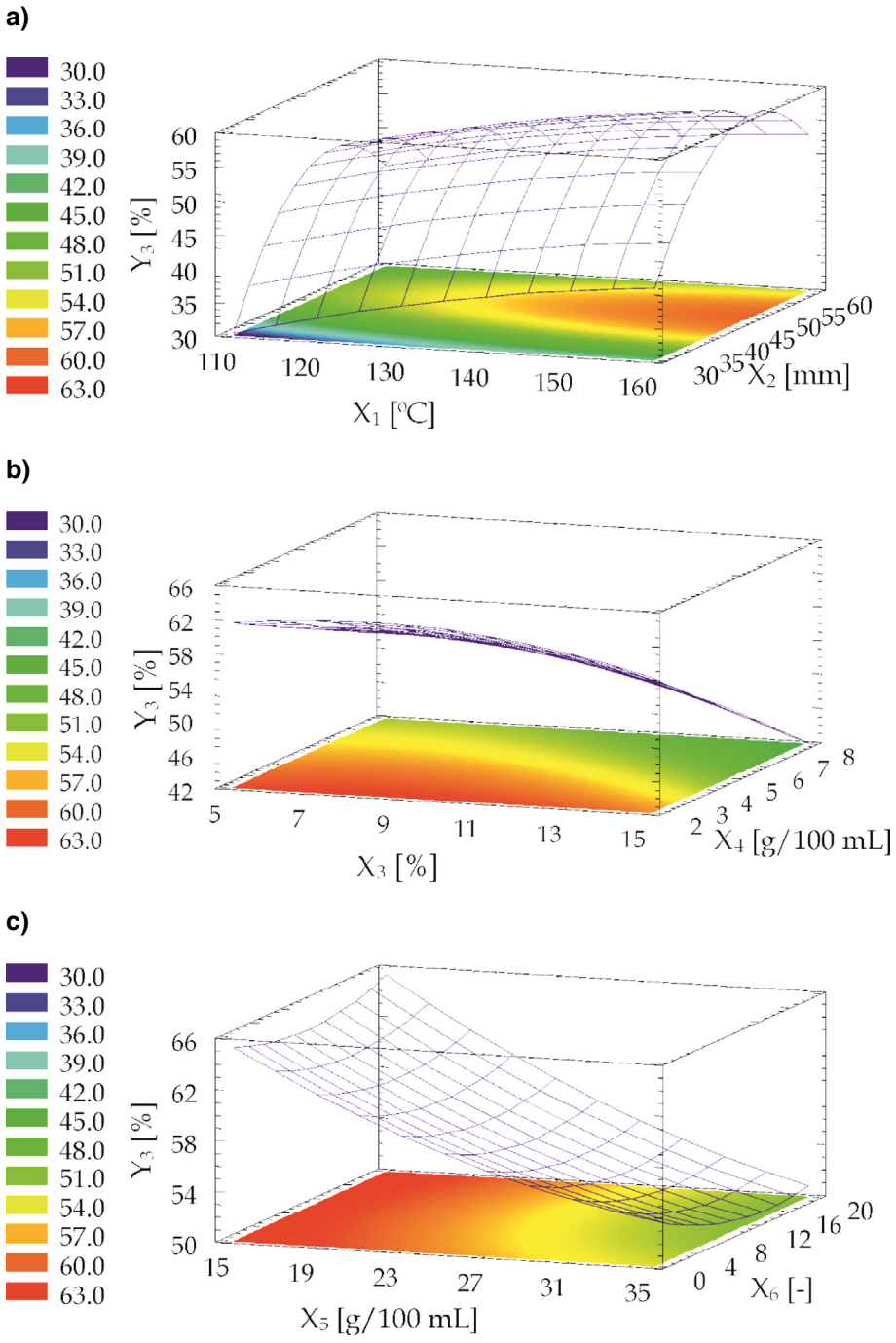

Fig. 3. Response surface plots showing the variation of the phytosterols retention against: a) inlet temperature (X_1) and air atomization flowrate (X_2); b) feed flowrate (X_3) and phytosterols content (X_4); c) total solids content (X_5) and AG to MD mass ratio (X_6).

microparticles (Fig. 2b). Carmona et al. [38] found similar effects in the microencapsulation of essential orange oil. In addition, the feed viscosity increased with the PS content, leading to bigger droplet and particle sizes.

The feed viscosity is also affected by the total solids content, particularly at low solids concentration. At these conditions, an increase in X_5 led to bigger microparticles probably due to the bigger droplets as a consequence of higher feed viscosities (Fig. 2c). The quadratic term of this factor (X_5^2) became evident at high values where an increase in X_5 led to a diminution in particle size because of a decrease in process yield by sticking. As afore-mentioned, bigger droplets tend to form a bigger atomization cone, so they can collide with the chamber walls near the entrance (i.e. when they are not completely dried) [24]. Thus, bigger droplets and particles tend to be retained on the dryer walls, diminishing the mean particle size of the collected particulate product. Di Battista et al. [19] explained these results by comparing the particle size distributions of the initial population (feed suspension), final product (microparticles) and material stuck on the chamber.

Finally, the mass ratio between AG and MD had a less significant linear effect on the mean size of the product microparticles (Fig. 2c). An increase in X_6 lead to smaller microparticles probably due to the lower surface tension of the resulting feed suspension [19,39,40].

3.3. Phytosterols retention (Y_3)

Phytosterols retention was between 20.50% (run 15) and 85.56% (run 44), being frequently lower than the corresponding process yields. Since phytosterols are non-volatile compounds, losses in spray drying are mainly by sticking on the dryer walls and drag by the exhaust air downstream to the cyclone. Accordingly, the difference between process yield and phytosterols retention for each experiment suggests a selective deposition of phytosterols on the chamber walls.

As it can be seen in Table 3, excepting the feed flowrate and the mass ratio between AG and MD, all the factors were significant on the phytosterols retention ($p < 0.05$). Moreover, the quadratic term of the

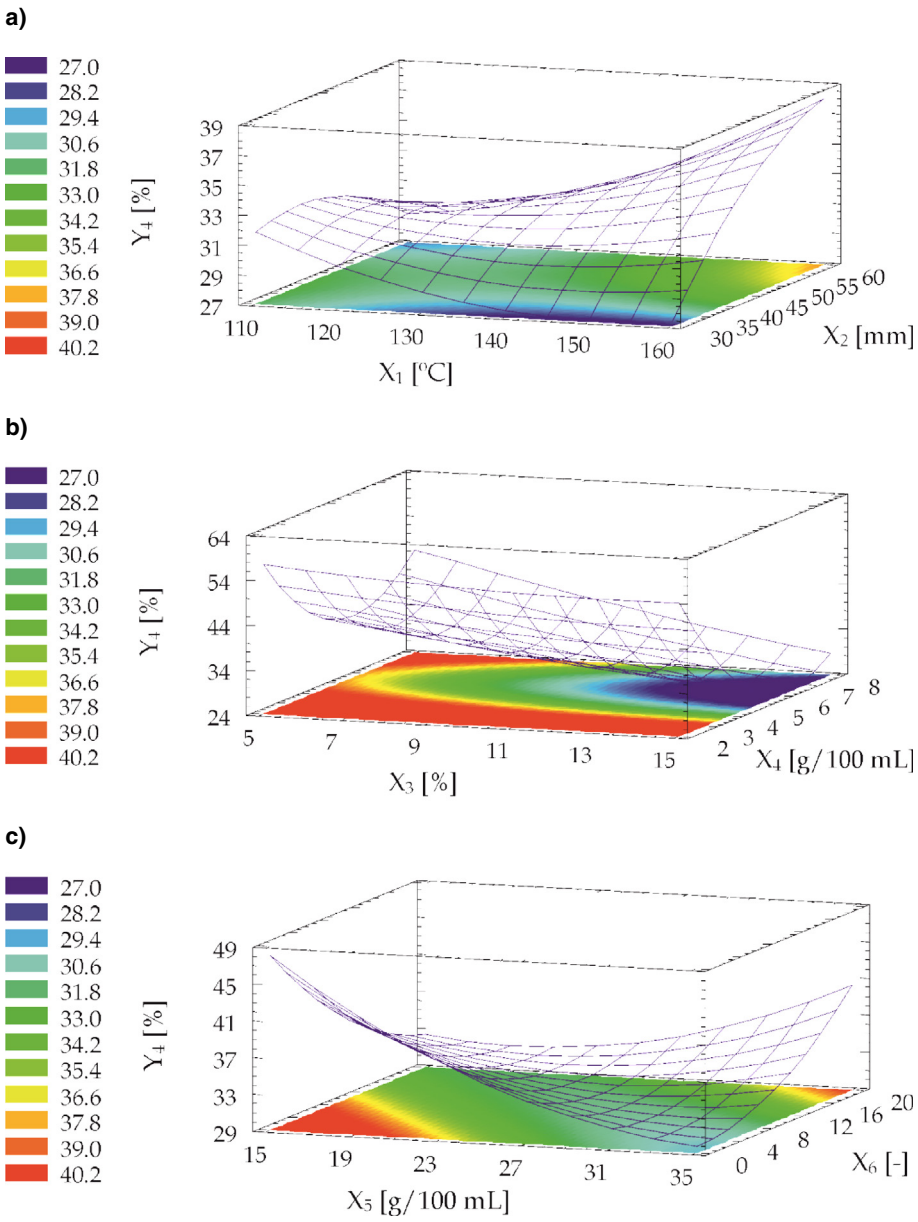

Fig. 4. Response surface plots showing the variation of the encapsulation efficiency against: a) inlet temperature (X_1) and air atomization flowrate (X_2); b) feed flowrate (X_3) and phytosterols content (X_4); c) total solids content (X_5) and AG to MD mass ratio (X_6).

Table 5
Criteria for the optimization of the responses in the microencapsulation of phytosterols.

	Lower limit	Upper limit	Goal
X_1: Inlet temperature (T_{in}) [°C]	110	160	
X_2: Atomization flowrate (Q_{atom}) [mm]	30	60	
X_3: Feed flowrate (Q_{feed}) [%]	5	15	
X_4: PS content ($Cont_{PS}$) [g/100 mL]	2	8	
X_5: Total solids content ($Cont_{TS}$) [g/100 mL]	15	35	
X_6: Mass ratio AG to MD (AG/MD) [−]	1/19	19/1	
Y_1: Process yield (PY) [%]	25.2	86.72	Maximize
Y_2: Mean size of product microparticles (D [4,3]$_{Part}$) [μm]	6.083	16.717	Minimize
Y_3: Phytosterols retention (PR) [%]	20.5	85.56	Maximize
Y_4: Encapsulation efficiency (EE) [%]	9.88	78.06	Maximize

Table 6
Optimal conditions for the phytosterols microencapsulation, predicted values and interval of confidence for all responses of interest.

	Optimum	
	Predicted	Interval of confidence
X_1: Inlet temperature (T_{in}) [°C]	160	
X_2: Atomization flowrate (Q_{atom}) [mm]	42	
X_3: Feed flowrate (Q_{feed}) [%]	7	
X_4: PS content ($Cont_{PS}$) [g/100 mL]	2	
X_5: Total solids content ($Cont_{TS}$) [g/100 mL]	15	
X_6: Mass ratio AG to MD (AG/MD) [−]	2.0575	
Y_1: Process yield (PY) [%]	84.36	77.93–90.75
Y_2: Mean size of product microparticles (D [4,3]$_{Part}$) [μm]	5.491	4.215–6.767
Y_3: Phytosterols retention (PR) [%]	76.59	61.31–91.87
Y_4: Encapsulation efficiency (EE) [%]	72.34	53.65–91.03

atomization air flowrate (X_2^2) and the interaction between AG to MD mass ratio and feed flowrate (X_3X_6) were also significant.

The model regression coefficients (Table 4) explained at 77.87% the data variability (R^2), whereas the lack of fit test was negative and the p-value of model was lower than 0.05, indicating that the model was appropriate.

Fig. 3 shows the response surfaces for the phytosterols retention (Y_3) as a function of the independent factors. The inlet temperature had a linear positive effect (Fig. 3a), possibly related with the high process yields obtained at high temperatures that improve the solids recovery. Similar results were obtained by Shiga et al. [41] in the encapsulation of *Lenthinus edodes*. The atomization air flowrate was the more influent factor on this response, particularly by its quadratic term (X_2^2) (Fig. 3a). As for the process yield, for low X_2 values, a positive effect was observed; while for high X_2 values, the effect was negative. For high atomization air flowrates, both the losses by sticking and drag were high [42].

The content of phytosterols and total solids in the feed had a linear negative effect on the phytosterols retention (Fig. 3b and c, respectively), probably related with the variations observed in the mean microparticle sizes.

3.4. Encapsulation efficiency (Y_4)

Finally, the encapsulation efficiency was between 9.88% (run 4) and 78.06% (run 30). This response was significantly affected just by the feed flowrate, the phytosterols content in its linear and quadratic terms and by its interaction with the total solids content (Table 3).

As it can be seen in Table 4, the regression coefficients indicate that the model for the encapsulation efficiency is appropriate; with a suitable R^2 value of 72.65%, without lack of fit ($p > 0.05$) and a p_{MOD} value lower than 0.05.

Fig. 4 shows the response surfaces for the encapsulation efficiency. Both, the effects of inlet temperature and atomization air flowrate were not significant on this response (Fig. 4a) in comparison with the other factors. Fig. 4b presents the adjusted encapsulation efficiency in terms of the feed flowrate (X_3) and phytosterols content (X_4). This response was improved by diminishing the feed flowrate. Wang et al. [16] observed similar trends in the microencapsulation of curcumin pigments. Moreover, the encapsulation efficiency was increased at low phytosterols concentrations, probably due to the lower microparticle sizes [19]. A comparable effect was observed by Aghbashlo et al. [43] in the microencapsulation of fish oil. The encapsulation efficiency shown a minimum against the phytosterols content, being the Y_4 value at the higher studied X_4 lower than that obtained at the lower assayed X_4.

3.5. Global optimization and validation

Based on the fitted models of each response, the desired goals and optimization limits reported in Table 5 (which were chosen according to the experimental results), global optimization was performed. Table 6 shows the optimal conditions that allow simultaneous optimization of the selected responses, together with the confidence interval for each one. Thereby, setting the inlet temperature at 160 °C, the atomization air flowrate at 498 L/h (equivalent to 42 mm of the rotameter height), the feed flowrate at 2.5 mL/min (equivalent to 7% of the pump capacity), the phytosterols and total solids contents at 2 and 15 g/100 mL, respectively and the AG to MD mass ratio at 2.0575, it was expected a process yield between 77.93 and 90.75%, a mean volume microparticle size within 4.215 and 6.767 μm, a phytosterols retention between 61.31 and 91.87% and an encapsulation efficiency within 53.65 and 91.03%.

Two experiments were run at these the optimal formulation and operating conditions and the obtained results were compared with the corresponding predicted values. All the experimental responses were

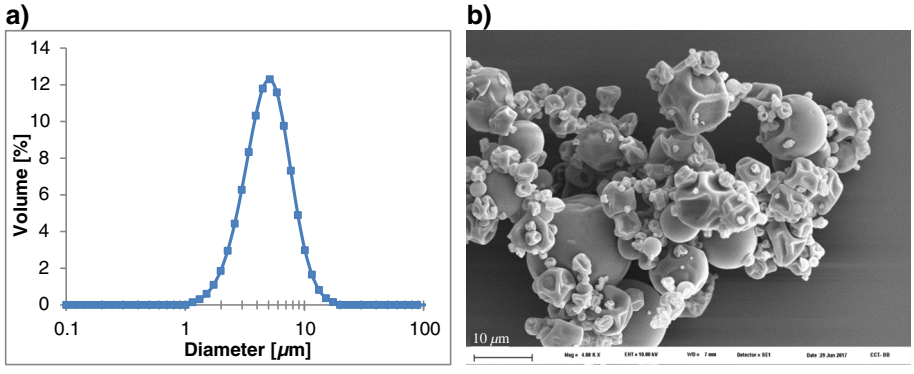

Fig. 5. a) Particle size distribution of the powder obtained under optimal conditions; b) Scanning electron micrograph of the same powder taken at 4000×.

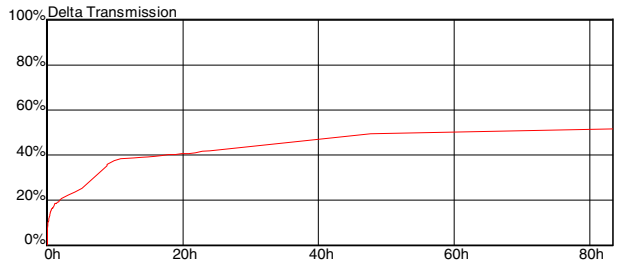

Fig. 6. Mean value of the delta transmission in the middle zone (9 to 50 mm) for the aqueous dispersion of raw phytosterols.

in good agreement with the predicted ones, being the process yield 81.73% ± 0.39%, the mean volume size of product microparticles 4.827 μm ± 0.090 μm (Fig. 5) and the phytosterols retention and encapsulation efficiency of 84.62% ± 1.39% and 68.30% ± 7.99%, respectively.

3.5.1. Particle morphology of optimal powder

Fig. 5 shows the particle size distribution and the SEM micrograph of the microparticles obtained under the optimal conditions. The product size distribution is unimodal (Fig. 5a), and the powder appears as ballooned particles which are surrounded by wrinkled and smaller ones (Fig. 5b). According to previous results, the arabic gum and maltodextrin seem to be deformed and dented spheres with smooth and shriveled surfaces, respectively [19]; being in agreement with the bigger particles that can be seen in the micrograph. Moreover, the SDS microparticles can be distinguished from the powder as irregular and considerable smaller [19].

3.5.2. Dispersibility and physical stability

Phytosterols are highly hydrophobic components with a density lower than water. Then, and as expected, they concentrated in the creamed phase of the aqueous suspension (Fig. S5). The phase separation occurred so fast that the transmittance in the top zone fell to zero instantaneously. Then, in the middle zone (from 9 mm to 50 mm) the transmittance increased to about 50%, due to lower concentration of raw phytosterols. Fig. 6 shows the time's variation of the average value of the transmission percentage in the middle zone of the tube (9 to 50 mm). As it can be seen, the mean transmission increased not only because of creaming but also due to an aggregation phenomenon that led to bigger particles. As the number of particles diminished due to agglomeration, the increments in the transmission became smaller and an almost constant was reached.

Regarding the optimal microparticles dispersed in water, the creamed and precipitated phases were also observed (Fig. S6). The

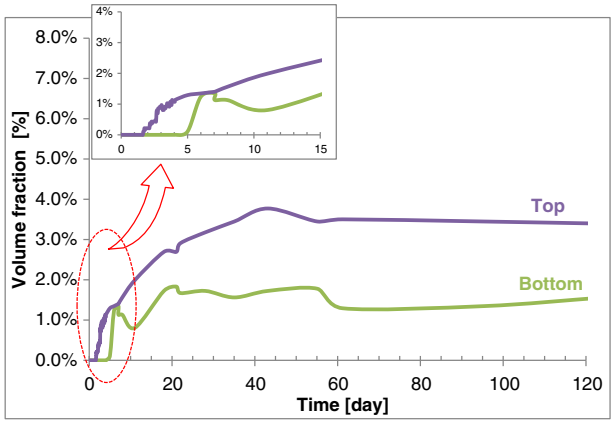

Fig. 7. Time evolution of the precipitated and creamed phases for the optimal microparticles suspended in water.

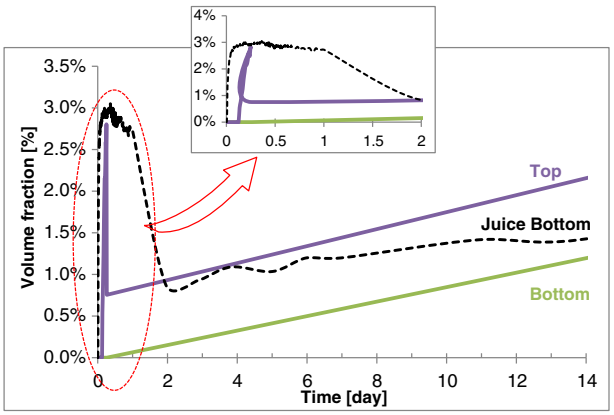

Fig. 8. Time evolution of precipitated and creamed phases for the optimal microparticles dispersed in the fruit juice, and time evolution of the precipitated phase inherent to the fruit juice beverage.

precipitated phase became visible at the bottom zone (at 8 mm, approximately; Fig. S6) after 4 days and it gradually increased up to 1.56% of the total volume of the sample (Fig. 7). The creaming phase was observed in the top zone (>60 mm, Fig. S6), after 1.5 days and evolved up to approximately 3.39% of the total volume of the sample (Fig. 7).

To analyze the behavior of the optimal microparticles dispersed in the instant beverage, the beverage without microparticles was first studied. For the pure juice, the profiles of backscattered and transmitted light shown a precipitated phase and its corresponding clarification zone at the top (without delimited phase) (Fig. S7). Thus, the fruit drink was unstable from the beginning, being the precipitated phase about 3% of the total volume (Fig. 8). After approximately 2 days, the volume fraction decreased to 1% indicating that the precipitated phase was labile during the first 2 days. After that, the volume fraction remained constant.

Fig. 8 also shows the time variation of the precipitated and creamed phases for the suspension of the optimal microparticles in the fruit juice. The corresponding transmission and backscattering profiles are shown in Fig. S8. This system was more unstable than that of the optimal microparticles redispersed in water; indeed, the development of the phases was faster probably due to the inherent instability of the instant fruit juice. Nevertheless, the addition of the optimal microparticles to the fruit juice delayed the precipitation process up to 17 h, showing a positive effect on the stability compared to the beverage without the microparticles. For the suspension of the optimal microparticles in the fruit juice, the oscillations in the volume fraction corresponding to the creamed phase indicated that it was labile and could be easily redispersed.

Moreover, it is important to note that the time required for redispersion of the optimal microparticles in water and in the beverage at 750 rpm was lower than one minute (between 40 and 50 s).

According to these results, the optimum powder containing phytosterols can be successfully applied in aqueous systems, delaying the migration phenomena with respect to raw phytosterols and improving the stability of the fruit juice beverage.

4. Conclusions

According to a Box-Behnken design of experiments, fifty four experiences were used to study the microencapsulation of phytosterols by spray drying in order to model and globally optimize the process performance and product quality. The study was carried out at 3 levels of drying air inlet temperature, atomization air flowrate, feed flowrate, phytosterols and total solids contents and mass ratio between wall materials (Arabic gum and maltodextrin). Response surface methodology was used to find an optimum set of formulation and operating

conditions in terms of process yield, mean volume size of product microparticles, phytosterols retention and encapsulation efficiency.

The effect of the studied formulation and operating variables was thoroughly analyzed. The atomization air flowrate was one of the most important factors, affecting significantly the process yield and phytosterols retention. Moreover, the phytosterols content was the main factor on the mean microparticle size and the encapsulation efficiency.

Taking into account the observed results and the analysis of variance, all the responses were successfully adjusted by a second order model with interactions. The obtained models shown good R^2 values and correlated the experimental data properly. Thus, the models were used to find an optimum set of formulation and operating conditions, which simultaneously allows maximum process yield, phytosterols retention and encapsulation efficiency and minimum mean volume size of product microparticles. The optimum set was experimentally validated. The microparticles corresponding to the optimal point were successfully applied in two aqueous systems (water at room temperature and a fruit drink instant beverage), giving stable products.

Acknowledgement

The authors thank to Agencia Nacional de Promoción Científica y Tecnológica (ANPCyT, Argentina) (PICT 2007-01147), Consejo Nacional de Investigaciones Científicas y Técnicas (CONICET, Argentina) (PIP 112-2008 01-01856, PIP 112-2011-0100336 112) and Universidad Nacional del Sur (UNS, Argentina) (PGI 24/M107, PGI 24/M122) for the financial support. Also, the authors thank to Daiana Trapé for the technical support performing the experiments.

C.A. Di Battista is special grateful to CONICET for the PhD fellowship and to Grupo Saporiti and Cooperativa Obrera for the donation of Arabic gum and phytosterols powder, respectively.

Appendix A. Supplementary data

Supplementary data to this article can be found online at http://dx.doi.org/10.1016/j.powtec.2017.08.008.

References

[1] P.A. da Costa, C.A. Ballus, J. Teixeira-Filho, H.T. Godoy, Phytosterols and tocopherols content of pulps and nuts of Brazilian fruits, Food Res. Int. 43 (2010) 1603–1606.
[2] P.C. Dutta, L. Normen, Capillary column gas – liquid chromatographic separation of D5-unsaturated and saturated phytosterols 1, J. Chromatogr. A 816 (1998) 177–184.
[3] P. Fernandes, J.M.S. Cabral, Phytosterols: applications and recovery methods, Bioresour. Technol. 98 (2007) 2335–2350.
[4] M.J. Lagarda, G. García-Llatas, R. Farré, Analysis of phytosterols in foods, J. Pharm. Biomed. Anal. 41 (2006) 1486–1496.
[5] R. Engel, H. Schubert, Formulation of phytosterols in emulsions for increased dose response in functional foods, Innovative Food Sci. Emerg. Technol. 6 (2005) 233–237.
[6] W.C. Franke, Compositions and Methods to Deliver Consumable Water Dispersible Phytosterols, WO 2006/062699, 2006.
[7] A.L. Thakkar, E.R. Diller, Pharmaceutical Dispersible Powder of Sitosterols and a Method for the Preparation Thereof, US 3881005, 1975.
[8] N. Auriou, Water-dispersible Encapsulated Sterols, US 2003/0165572 A1, 2003.
[9] H. Auweter, H. Bohn, O. Hasselwander, F. Runge, Process for Producing Pulvurulent Phytosterols Formulations, US 2009/0047355 A1, 2009.
[10] A. Gharsallaoui, G. Roudaut, O. Chambin, A. Voilley, R. Saurel, Applications of spray-drying in microencapsulation of food ingredients: an overview, Food Res. Int. 40 (2007) 1107–1121.
[11] A. Matalanis, O.G. Jones, D.J. McClements, Structured biopolymer-based delivery systems for encapsulation, protection, and release of lipophilic compounds, Food Hydrocoll. 25 (2011) 1865–1880.
[12] T. Sartori, L. Consoli, M.D. Hubinger, F.C. Menegalli, Ascorbic acid microencapsulation by spray chilling: production and characterization, LWT Food Sci. Technol. 63 (2015) 353–360.
[13] C. Turchiuli, M. Fuchs, M. Bohin, M.E. Cuvelier, C. Ordonnaud, M.N. Peyrat-Maillard, E. Dumoulin, Oil encapsulation by spray drying and fluidised bed agglomeration, Innovative Food Sci. Emerg. Technol. 6 (2005) 29–35.
[14] E.C. Frascareli, V.M. Silva, R.V. Tonon, M.D. Hubinger, Effect of process conditions on the microencapsulation of coffee oil by spray drying, Food Bioprod. Process. 90 (2012) 413–424.
[15] B.N. Estevinho, F. Rocha, L. Santos, A. Alves, Microencapsulation with chitosan by spray drying for industry applications - a review, Trends Food Sci. Technol. 31 (2013) 138–155.
[16] Y. Wang, Z. Lu, F. Lv, X. Bie, Study on microencapsulation of curcumin pigments by spray drying, Eur. Food Res. Technol. 229 (2009) 391–396.
[17] J. Smith, E. Charter, Functional Food Product Development, Wiley-Blackwell, Oxford, United Kingdom, 2010.
[18] M.V. Bule, R.S. Singhal, J.F. Kennedy, Microencapsulation of ubiquinone-10 in carbohydrate matrices for improved stability, Carbohydr. Polym. 82 (2010) 1290–1296.
[19] C.A. Di Battista, D. Constenla, M.V. Ramírez-Rigo, J. Piña, The use of arabic gum, maltodextrin and surfactants in the microencapsulation of phytosterols by spray drying, Powder Technol. 286 (2015) 193–201.
[20] J.A. Gallegos-Infante, N.E. Rocha-Guzmán, R.F. González-Laredo, L. Medina-Torres, C.A. Gomez-Aldapa, L.A. Ochoa-Martínez, C.E. Martínez-Sánchez, B. Hernández-Santos, J. Rodríguez-Ramírez, Physicochemical properties and antioxidant capacity of oak (*Quercus resinosa*) leaf infusions encapsulated by spray-drying, Food Biosci. 2 (2013) 31–38.
[21] M.C. Otálora, J.G. Carriazo, L. Iturriaga, M.A. Nazareno, C. Osorio, Microencapsulation of betalains obtained from cactus fruit (*Opuntia ficus-indica*) by spray drying using cactus cladode mucilage and maltodextrin as encapsulating agents, Food Chem. 187 (2015) 174–181.
[22] J. Velasco, F. Holgado, C. Dobarganes, G. Márquez-Ruiz, Antioxidant activity of added phenolic compounds in freeze-dried microencapsulated sunflower oil, J. Am. Oil Chem. Soc. 86 (2009) 445–452.
[23] T. Zhang, B.-B.C. Youan, Analysis of process parameters affecting spray-dried oily core nanocapsules using factorial design, AAPS PharmSciTech 11 (2010) 1422–1431.
[24] A.M. Goula, K.G. Adamopoulos, Spray drying performance of a laboratory spray dryer for tomato powder preparation, Dry. Technol. 21 (2003) 1273–1289.
[25] Y.Z. Cai, H. Corke, Production and properties of spray-dried *Amaranthus betacyanin* pigments, J. Food Sci. 65 (2000) 1248–1252.
[26] T.C. Kha, M.H. Nguyen, P.D. Roach, C.E. Stathopoulos, Microencapsulation of Gac oil: optimisation of spray drying conditions using response surface methodology, Powder Technol. 264 (2014) 298–309.
[27] P. Roccia, M.L. Martínez, J.M. Llabot, P.D. Ribotta, Influence of spray-drying operating conditions on sunflower oil powder qualities, Powder Technol. 254 (2014) 307–313.
[28] R.V. Tonon, C. Brabet, M.D. Hubinger, Influence of process conditions on the physicochemical properties of açai (*Euterpe oleraceae* Mart.) powder produced by spray drying, J. Food Eng. 88 (2008) 411–418.
[29] K. Anekella, V. Orsat, Optimization of microencapsulation of probiotics in raspberry juice by spray drying, LWT Food Sci. Technol. 50 (2013) 17–24.
[30] P. Kaur, S.K. Singh, V. Garg, M. Gulati, Y. Vaidya, Optimization of spray drying process for formulation of solid dispersion containing polypeptide-k powder through quality by design approach, Powder Technol. 284 (2015) 1–11.
[31] B. Adhikari, T. Howes, B.J. Wood, B.R. Bhandari, The effect of low molecular weight surfactants and proteins on surface stickiness of sucrose during powder formation through spray drying, J. Food Eng. 94 (2009) 135–143.
[32] I. Tontul, A. Topuz, Influence of emulsion composition and ultrasonication time on flaxseed oil powder properties, Powder Technol. 264 (2014) 54–60.
[33] C.A. Di Battista, D. Constenla, J. Piña, M.V. Ramírez Rigo, Influencia del contenido y tipo de tensoactivo en la microencapsulación de fitoesteroles, IV Congr. Int. Cienc. Y Tecnol. Los Aliment., Córdoba, 2012.
[34] L. Gallo, J.M. Llabot, D. Allemandi, V. Bucalá, J. Piña, Influence of spray-drying operating conditions on *Rhamnus purshiana* (Cáscara sagrada) extract powder physical properties, Powder Technol. 208 (2011) 205–214.
[35] P. Mishra, S. Mishra, C.L. Mahanta, Effect of maltodextrin concentration and inlet temperature during spray drying on physicochemical and antioxidant properties of amla (Emblica officinalis) juice powder, Food Bioprod. Process. 92 (2014) 252–258.
[36] S. Drusch, K. Schwarz, Microencapsulation properties of two different types of n-octenylsuccinate-derivatised starch, Eur. Food Res. Technol. 222 (2006) 155–164.
[37] R.V. Tonon, C.R.F. Grosso, M.D. Hubinger, Influence of emulsion composition and inlet air temperature on the microencapsulation of flaxseed oil by spray drying, Food Res. Int. 44 (2011) 282–289.
[38] P.A.O. Carmona, R.V. Tonon, R.L. da Cunha, M.D. Hubinger, Influence of emulsion properties on the microencapsulation of orange essential oil by spray drying, J. Colloid Sci. Biotechnol. 2 (2013) 130–139.
[39] Z. Wang, G. Narsimhan, D. Kim, Characterization of the effect of food emulsifiers on contact angle and dispersibility of lipid coated neutrally buoyant particles, LWT Food Sci. Technol. 41 (2008) 1232–1238.
[40] A.P. Tinke, R. Govoreanu, I. Weuts, K. Vanhoutte, D. De Smaele, A review of underlying fundamentals in a wet dispersion size analysis of powders, Powder Technol. 196 (2009) 102–114.
[41] H. Shiga, H. Yoshii, H. Ohe, M. Yasuda, T. Furuta, H. Kuwahara, M. Ohkawara, P. Linko, Encapsulation of shiitake (Lenthinus edodes) flavors by spray drying, Biosci. Biotechnol. Biochem. 68 (2004) 66–71.
[42] A. Sosnik, K.P. Seremeta, Advantages and challenges of the spray-drying technology for the production of pure drug particles and drug-loaded polymeric carriers, Adv. Colloid Interf. Sci. 223 (2015) 40–54.
[43] M. Aghbashlo, H. Mobli, A. Madadlou, S. Rafiee, The correlation of wall material composition with flow characteristics and encapsulation behavior of fish oil emulsion, Food Res. Int. 49 (2012) 379–388.